

DIFFUSION ON SEMICONDUCTOR SURFACES

Semiconductor devices continue to get ever smaller, which means that individual defects play an increasingly important role in their performance. In the process of fabricating more innovative, better performing devices, crystal growers have developed an amazing intuition about how atoms and molecules behave on crystal surfaces. Their intuition, formed from knowledge of fundamental atomic-scale processes and honed through experience, concerns such questions as where atoms and molecules stick, how they interact with each other and the substrate, and how they diffuse.

Atomic and molecular diffusion, in particular, have important effects on such processes as crystal growth, etching, chemical reactions, and the stability of nanostructures. (See the PHYSICS TODAY articles “A Surface View of Etching” by John J. Boland and John H. Weaver, August 1998, page 34 and “Nanoscale Fluctuations at Solid Surfaces” by Zoltán Toroczkai and Ellen D. Williams, December 1999, page 24.) For example, the evolution of smooth surfaces during crystal growth requires that randomly deposited atoms diffuse to step edges where they can be incorporated.

We consider diffusion, and also binding and atomic interactions, for the relatively simple model system of silicon dimers on the Si(001) surface. Silicon is intensely studied because of its importance in the microelectronics industry,¹ and its (001) surface displays a wealth of fascinating phenomena.² When a Si crystal is cut along the (001) plane, each surface atom is left with two dangling bonds. The surface reconstructs to form rows of dimerized atoms, yielding a (2×1) unit cell; the driving force for reconstruction is the reduction in the number of dangling bonds from two to one. When an individual Si atom is deposited onto the surface at room temperature, it diffuses

Atomic-resolution imaging techniques show that a good deal of surface physics can be understood with elementary statistical mechanics, but some surprisingly complex behaviors occur even in simple systems.

Harold J. W. Zandvliet, Bene Poelsema,
and Brian S. Swartzentruber

rapidly and quickly finds another atom with which to form an adsorbed dimer. Adsorbed dimers can be bound either on top of, or between, the substrate dimer rows and can have their dimer bonds oriented parallel or perpendicular to the rows. Dimers on top of the substrate rows can rotate, changing their orientation from parallel to perpendicular and back. They can also diffuse, both along and across substrate rows. The stability of binding sites, along with rotational and diffusion barriers, can all be readily extracted from real-time scanning tunneling microscopy (STM) experiments—with the help of elementary statistical mechanics—to give a map of the atomic-scale potential energy landscape.

Settling into binding sites

Silicon dimers adsorbed onto the Si(001) surface appear as bright bumps in an STM image, as shown in figure 1. The four possible bound configuration states described previously are illustrated and labeled A, B, C, and D in figure 2, which also shows STM images for the two on-top adsorption states A and B.

Each of the four configuration states has a different bound-state energy. In equilibrium, the relative populations of the adsorbed dimers in each configuration state reflect their bound-state energies as given by the Boltzmann factor. For example, the number of adsorbed dimers in state A divided by those in state B is equal to $\exp(-(E_A - E_B)/kT)$, where E_A and E_B are the bound-state energies. The majority of the adsorbed dimers are observed to bind in state B, implying that this state is the lowest-energy binding configuration. The second most populous is state A, with C third. Isolated dimers in configuration D have not been observed, perhaps because the three-dimensional structure of the Si(001) surface creates energy barriers that cannot be overcome at the temperatures of the experiments (300–450 K). At room temperature, with kT equal to 26 meV, about 10 times more adsorbed dimers are observed in state B than in state A, implying a bound-state energy difference of 60 meV. Because the population ratio depends exponentially on energy, a small difference in the bound-state energies has a large effect on the relative state populations.

HAROLD ZANDVLIET is an associate professor in the department of applied physics and a scientific staff member of the MESA+ research institute and BENE POELSEMA is a professor in the department of applied physics and a scientific staff member of MESA+ at the University of Twente, in Enschede, the Netherlands. BRIAN SWARTZENTRUBER is a principal member of the technical staff at Sandia National Laboratories in Albuquerque, New Mexico.

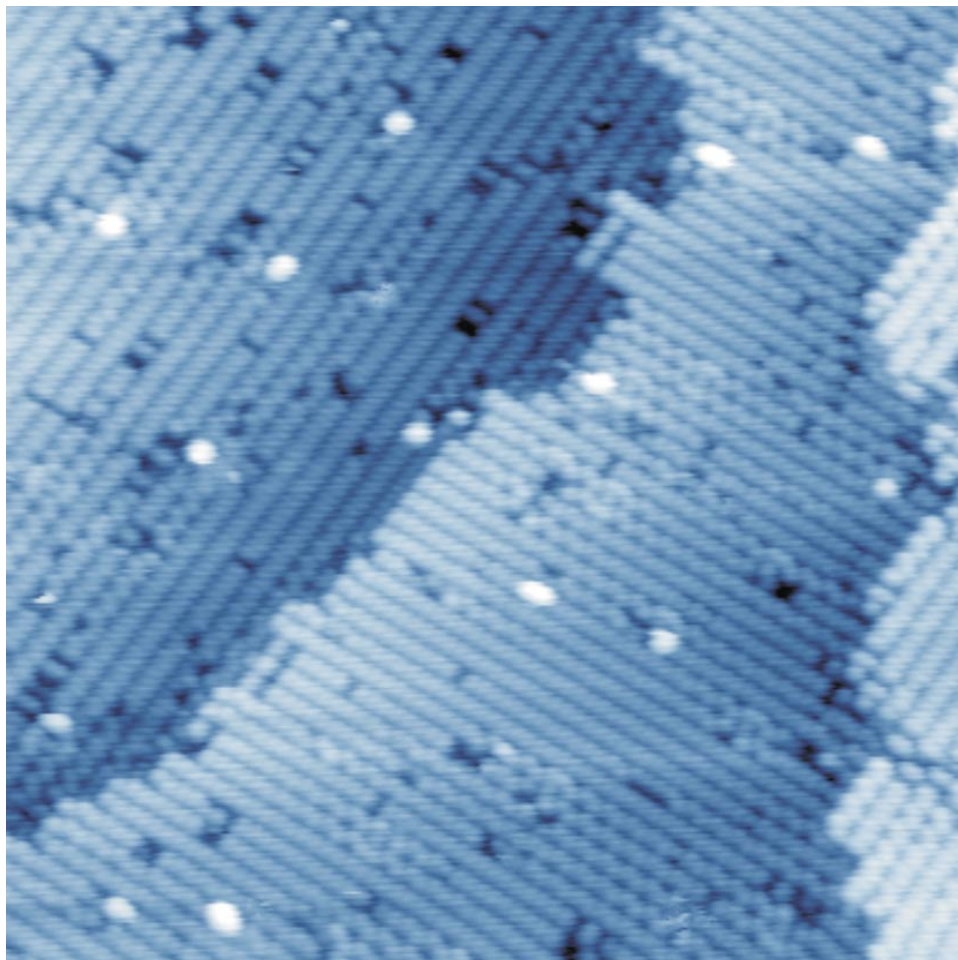


FIGURE 1. A SCANNING tunneling microscope image of a silicon (001) surface after the deposition of a small amount of Si at room temperature. The image shows two single-layer steps (the jagged interfaces) separating three terraces. Because of the tetrahedral bonding configuration in the silicon lattice, dimer row directions are orthogonal on terraces joined by a single-layer step. The area pictured is 30×30 nm.

Configuration states A, B, and C all have appreciable occupation probabilities. Measuring these probabilities allows one to test theoretical calculations of relative bound-state energies. With improved algorithms developed since the mid-1980s and recent increases in computational power, it has become possible to perform *ab initio* electronic-structure calculations that take into account many more factors than was previously feasible. These calculations typically vary in the level of approximation used for such technical details as the number of

atoms independently treated in the calculation, the plane-wave kinetic-energy cutoff, the Brillouin k -point sampling, and whether a gradient correction is used. The less restrictive the approximations, the more computer power and time one needs to run a calculation. Therefore, it is crucial to determine whether decreasing the level of approximation leads to a significant change in the results of the computer run. For Si surface structures, it is possible to calculate absolute configuration energies to a precision of less than 100 meV and relative energies to somewhat better precision. The table on page 42 gives the results of several first-principles calculations of the relative bound-state energies of the four possible adsorbed-dimer binding configurations,³⁻⁵ along with experimental values,⁶⁻⁸ to illustrate the accuracy of the calculations.

Clearing rotational barriers

So far, the discussion has focused on equilibrium properties of the Si-on-Si system, which are governed solely by

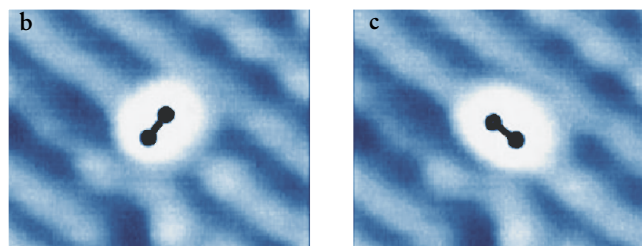
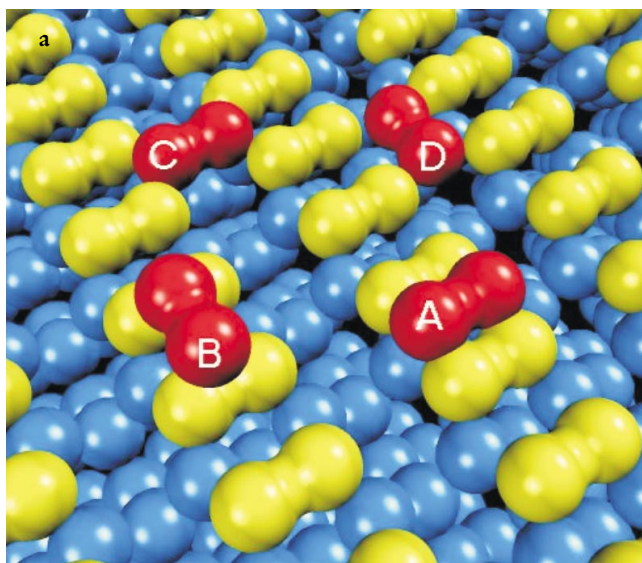


FIGURE 2. BOUND CONFIGURATIONS for silicon dimers on a Si(001) substrate. (a) Schematic in which blue balls represent the bulk atoms, yellow dumbbells represent the substrate dimers and red dumbbells represent the adsorbed dimers. The lower images show an adsorbed dimer (b) in the A state and (c) in the B state (adapted from ref. 18). Superimposed on these scanning tunneling microscope images are black dumbbells showing the position and orientation of the adsorbed dimer. The area pictured in the STM images is 4×3 nm.

bound-state energies—local minima in the potential energy landscape. Now consider the kinetics of the system, that is, how it evolves. As a system moves from one stable state to another, it passes through a so-called transition state. The rate at which one stable configuration changes to another depends on the temperature and the energy of the transition state according to the Arrhenius relation $\nu = \nu_0 \exp(-E/kT)$. Here, E is the activation barrier, that is, the difference in energy between the transition state and the original stable state. The prefactor ν_0 is called the attempt frequency, and may be thought of as the rate at which the original stable state attempts to cross the activation barrier.

At room temperature, an adsorbed dimer bound on top of the Si(001) surface will rotate between the orthogonal B and A states on a time scale on the order of a second.^{6,7} Figures 2b and 2c show a single dimer in each of these states. The rotation dynamics can be measured quantitatively using atom-tracking STM. In atom-tracking mode, the STM tip is locked over a selected dimer using lateral feedback. The average position of the tip is maintained over the adsorbed dimer while the x , y , and z coordinate feedback data are continuously recorded. (For more details, see the box below.) Because of differences in configuration and electronic structure between the A and B rotation states, the tip is closer to the surface over the A state than over the B state. Therefore, the rotation state of the adsorbed dimer is reflected in the height of the STM tip as a function of time, as displayed in figure 3a.

The energetics of the rotational-kinematics discussion are indicated by the potential energy surface schematically depicted in figure 3b. Of the two stable configuration states, state B is slightly favored over state A,

Configuration	BK ³	YUT ⁴	SJ1 ⁵	SJ2 ⁵	Experiment ⁶⁻⁸
A	-0.01	0.07	0.0-0.1	0.0-0.1	0.06 ± .01
B	0.00	0.00	0.00	0.00	0.00
C	0.30	0.18	0.20	0.50	0.061 ± .016
D	1.10	0.76	0.60	1.00	

BOUND-STATE ENERGIES in eV of the four possible adsorbed-dimer binding configurations on silicon (001), relative to that of state B. The columns giving theoretical results are labeled with the initials of the authors making the calculation. The authors of ref. 5 ran two calculations. The last experimental row is blank, reflecting the fact that isolated D dimers have yet to be observed. The calculated energies are zero-temperature configuration energies, whereas the measured values are at room temperature and therefore reflect degeneracies associated with the rocking of the adsorbed dimer. Thus, a comparison of the theoretical and empirical relative energies is not strictly justifiable, although it is generally believed that the temperature effects are small—or at least similar—for the different configurations at room temperature.

and therefore the activation barrier to go from A to B is lower than to go from B to A. Ideas from elementary statistical mechanics allowed determination of the energies displayed in the figure: The activation barriers were obtained using the Arrhenius relation, whereas the Boltzmann relation was used to determine the bound-state energy difference. The transition rates and relative populations are simply connected by the potential energy surface, using the concept of detailed balance.

Dissociating and recombining

Atomic-resolution imaging techniques, such as field ion microscopy and STM, have provided a remarkable look at the variety of ways in which atoms and small molecules diffuse on surfaces. Thermally activated diffusion from

Atom-Tracking Scanning Tunneling Microscopy

To study individual dynamic events in real space with a conventional scanning tunneling microscope, one collects images of the same area of the surface and then compares consecutive images to resolve atomic-scale events. The time resolution of this procedure is determined by the acquisition time of each individual image, which in turn is determined by the design characteristics of the microscope and the area of the image being scanned. Typical time resolutions for conventional STM range from one to several hundred seconds per image.

The technique of atom tracking dramatically improves this time resolution. While atom tracking, the STM tip is locked onto a selected atom or cluster using two-dimensional lateral feedback. The lateral feedback is accomplished by having the tip execute circular motion, generally a few angstroms in radius, at a frequency greater than the cutoff frequency of the z -feedback electronics. A lock-in amplifier measures the derivative of the tunnel current with respect to the lateral coordinates x and y . These derivatives are passed on to independent x and y integrating feedback circuits that maintain a position of zero local slope (that is, on top of the atom or cluster). The net result of the lateral feedback is to force the tip to continually climb uphill, following the local surface gradient and remaining at the top of the atom or cluster.

When an atom diffuses to a neighboring site on the surface, the tracking tip quickly relocates to the atom's new position. Atom-tracking STM can readily detect the double jumps that occur in trough diffusion, though larger jumps may not be observable. When an exchange event occurs, the atom tracker

loses sight of the originally targeted atom, but locks onto the exchanged atom that moves on top of the surface. By a simple inversion of the phases of the x and y feedback circuits, the atom tracker can be forced to run downhill in order to lock onto vacancies and surface depressions. In atom-tracking mode, the STM spends all of its time measuring the kinetics of the selected atom instead of acquiring a 2D image of its neighborhood. Thus, atom tracking dramatically improves the time resolution for measuring individual dynamic events by a factor of one thousand, typically to 5–50 milliseconds.

Species imaged during atom-tracking measurements can be subjected to very large electric fields and current densities because of the close proximity of the microscope tip to the sample, and the small lateral area over which electrons tunnel. This raises the possibility that the tunneling process itself can affect the measurements of activation barriers. By changing the applied bias voltage and the tip's lateral offset, one can systematically vary the tip-induced electric field in both magnitude and direction to determine how changing the electric field affects the measured barriers. Throughout the range of typical tunneling conditions, the activation barrier for rotation varies by less than 6%, with the variance depending quadratically on the field. The activation barrier for diffusion of a Si dimer on Si(001) varies by less than 3%, with the variation depending linearly on the field. Both activation barriers remain unchanged as the tunnel current varies over two orders of magnitude, therefore ruling out the possibility of electron-stimulated processes contributing to a change in kinetics.¹⁸

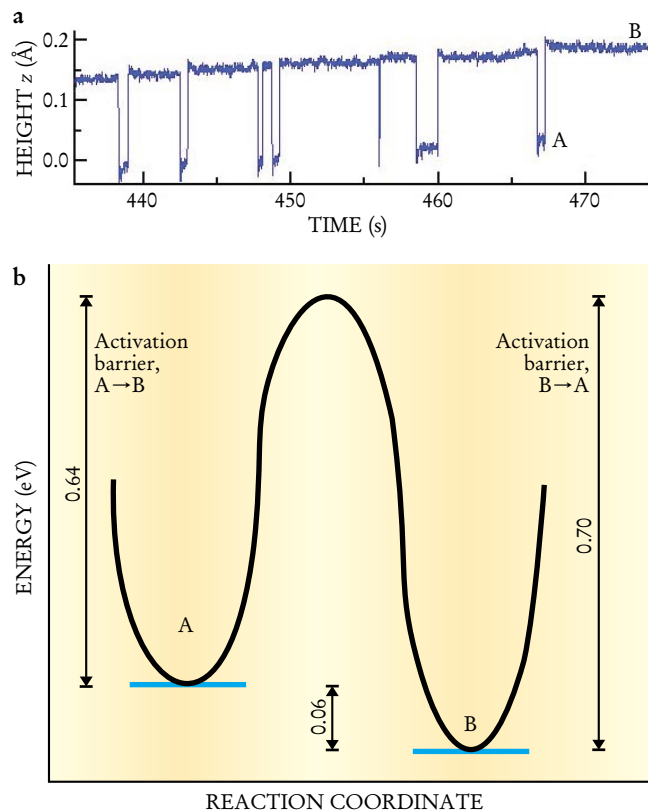


FIGURE 3. TRANSITIONS BETWEEN A AND B STATES. (a) The measured height, z , of a scanning tunneling microscope tip above an isolated dimer on a silicon surface as a function of time, showing the transitions between the A and B states. The dimer has a higher probability of being found in state B, a consequence of that configuration's lower bound-state energy. The different transition rates implied for the two states are reflected in their residence times, the periods spent in the given state before making a transition. The dimer has a much greater residence time in state B than in state A. The upward slope of the graph is an experimental artifact and reflects the fact that absolute heights cannot be reliably measured. Relative height differences between the A and B states, however, can be measured accurately. (Adapted from ref. 7.) (b) Potential energy surface connecting the A and B states. The reaction coordinate can be interpreted as the angle of the adsorbed dimer bond with respect to the substrate rows. Measurements such as those in (a), made as a function of temperature, yield the activation barriers.⁷ Occupation-probability measurements yield the bound-state energy separation.⁶ Consistent with the principle of detailed balance, the difference in activation barriers equals the difference in bound-state energies.

one substrate site to another can occur either by a simple hop mechanism or by an exchange mechanism in which an atom on top of a surface replaces an atom in the first layer of the surface, while the replaced atom moves to the on-top site. The atomic exchange mechanism was proposed by D. W. Bassett and P. R. Webber⁹ in 1978. Experimental confirmation came more than 10 years later, reported in papers simultaneously published by Gary Kellogg and Peter Feibelman,¹⁰ who considered platinum on platinum (001) and by Changlin Chen and Tien Tson¹¹ who studied iridium on iridium (001).

The variety of diffusion processes that can be observed is enhanced when the diffusing species is a dimer rather than a single atom. For instance, dimers can diffuse as a two-atom unit or one atom at a time. In the latter process, the two atoms of the dimer may recombine immediately after dissociating or they may move away from each other and continue to perform simultaneous one-dimensional random walks until they meet each other (or perhaps another wayward atom) and recombine.

Recent atom-tracking experiments¹² reveal that on-top dimers diffusing along Si(001) rows always hop to nearest-neighbor sites. This strongly suggests that the on-top dimer remains bound during diffusion. The same experiments show that dimer diffusion in the troughs of the Si substrate is quite different. In the valleys, dimers execute double and triple jumps quite frequently. These long jumps indicate that the dimer bond breaks and the two atoms move nearly independently along the trough until they meet again and recombine.

Another interesting phenomenon associated with trough diffusion has been observed in the germanium on germanium (001) system: diffusion-driven concerted motion of substrate atoms.¹³ The Ge(001) surface reconstructs to form rows of dimerized atoms just as the Si(001) surface does. When about 1% of a germanium monolayer

is deposited onto a Ge(001) surface at room temperature, isolated dimers at on-top as well as trough sites are found. As a trough dimer jumps to one of the neighboring trough sites, the substrate surface in the vicinity of the jump flexes visibly in response, as shown in figure 4. This motion belies the common impression that dimer diffusion leaves the substrate unaltered.

Clearing diffusion barriers

Atom-tracking STM has been used to measure the rate at which Si dimers hop along the top of Si substrate dimer rows,^{12,14} over temperatures ranging from room temperature to 460 K. For this row hopping, as opposed to the more complicated trough diffusion just discussed, the Arrhenius relation applies, as evidenced by the plot of the hop rate versus inverse temperature shown in figure 5. The figure indicates that, at room temperature, an adsorbed dimer hops about once or twice per hour, whereas at 400 K it hops about 10 times per second, an increase of about four orders of magnitude. The activation barrier extracted from the Arrhenius plot is slightly less than 1 eV.

Although the activation barrier for diffusion on top of substrate dimer rows is reliably known, measured hop rates at specific temperatures have differed by more than an order of magnitude.^{12,14} A likely source of at least some of the disagreement is the difficulty in measuring temperature, particularly in the range from slightly above room temperature to 470 K. A temperature uncertainty of ± 25 K would explain the measured discrepancies in hop rates cited in refs. 12 and 14. Fortunately, temperature uncertainties have a very small effect on *relative* energies, such as the difference in bound-state energies between two sites measured at a constant temperature. The greatest contributor to uncertainties in the measurement of relative energies is the standard root- N error of statistical measurements. With easily acquired data sets of several hundred measurements, uncertainties as small as 5 meV can be achieved.

One-dimensional diffusion along rows is a random walk: An adsorbed dimer is equally likely to hop to either of its nearest-neighbor sites. One can readily verify this by extracting the mean-square displacement from a

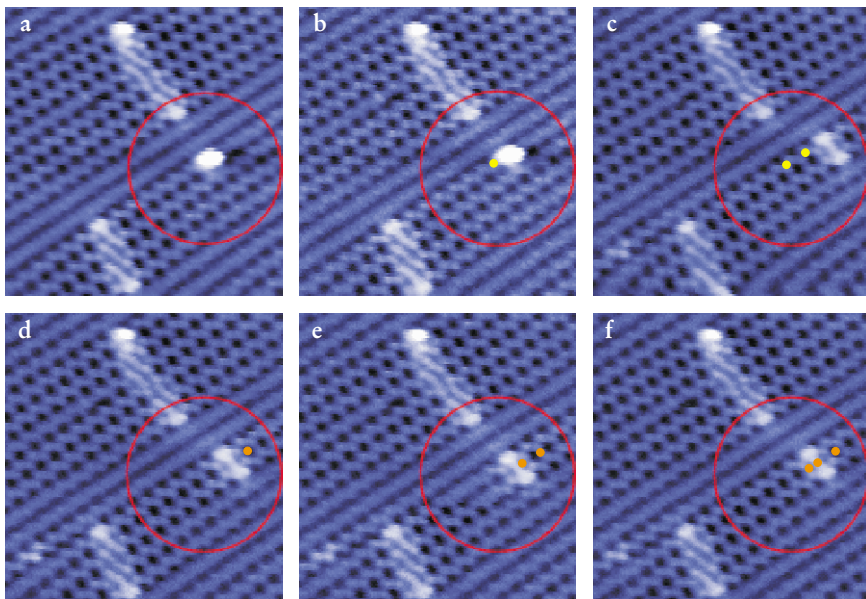
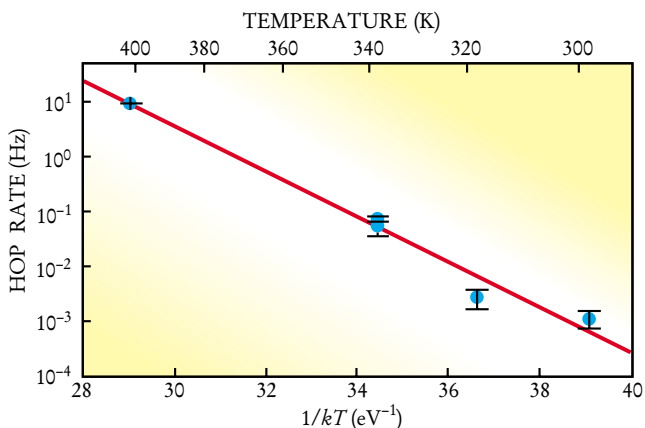


FIGURE 4. DIMER DIFFUSION IN GERMANIUM. The images are a series of room-temperature scanning tunneling microscope scans of a 10×10 -nm segment of a Ge(001) surface on which about 1% of a germanium monolayer was deposited. The time lapse between images is 276 seconds. The yellow and orange marks indicate the previous positions visited by the dimer. Initially the dimer was in the most-stable B configuration and diffused over one of the Ge substrate rows. By the time image (c) was taken, the dimer was in the C configuration, having rotated by 90° and hopped to a trough position between two substrate rows. In this image, some of the substrate rows in the vicinity of the diffusing dimer appear as dots of varying intensity—related to a buckling of the surface dimers in which one surface dimer atom is displaced out of the surface while the other is displaced inward. The specific pattern imaged in (c) indicates that neighboring dimers in the same row tend to buckle in opposite senses. As the dimer diffuses in the trough, its local environment changes significantly. Atoms originally displaced out of the surface become displaced inward and vice versa. In images (d), (e), and (f) these changes are manifested as a fading and reintensification of the buckling registry of the substrate rows in the vicinity of the diffusing dimer.

sequence of STM images and plotting it versus time. The relation is linear, as it should be.

Dimers can also hop between substrate dimer rows. The activation barrier for this process, however, is high enough that it is seen⁸ only at temperatures above about 450 K. At 450 K, an adsorbed dimer hops along the substrate dimer rows more than 100 times per second.¹⁴

Atom-tracking STM allows one to measure individual dynamic events occurring over time scales as short as 5 ms. Unfortunately, this is not good enough for an experi-



mental determination of the atomic pathway (a detailed description of the motion of the dimer's atoms that would indicate, in particular, whether the dimer bond breaks) for the diffusion and rotation processes. Part of the time, adsorbates are just sitting on the surface in metastable binding sites. Transitions occur rarely but rapidly—in about 10^{-12} seconds. That is much too fast to be measured experimentally, but not too fast to be analyzed theoretically.

Several recent *ab initio* calculations, though not definitive, do suggest possible atomic pathways for the rotation and diffusion of dimers. The calculated pathways differ in detail and are all quite complicated, but do, however, give activation barriers consistent with experiment. Such calculations are beginning to provide us with an intuitive picture of rotation and diffusion and are a step toward the goal of developing consistently reliable methods to predict atomic-scale behavior from first principles.

More complicated interactions

The silicon (001) surface contains interesting topographic features including steps, islands, and point defects. With STM, one can study the interactions of adsorbed atoms and dimers with such features. Point defects, for example, interact with adsorbates, affecting the way in which islands are formed during the process of crystal growth. In the absence of defects, the size and spacing of the islands can be controlled,

but defects can serve as obstacles for diffusion and as nucleation sites for islands beyond the control of crystal growers. In addition, STM allows one to measure specific energies such as the bound-state energies next to steps and islands, and the detailed potential energy landscape along a crystal step. The bound-state energies are key inputs for the construction of models designed to give insight into the process of crystal growth, while the potential energy landscape determines the locations along step edges where diffusing dimers can be incorporated.

The basic methods and concepts we have discussed in the context of the Si-on-Si system can be applied to much more complicated systems. Both Si and Ge are group IV elements and chemically similar. Nonetheless, there are a number of differences between Si-Ge systems and the homogeneous Si-on-Si system. For example, surface structures can form, the simplest of which is a Si-Ge adsorbed dimer. The different sized atoms that form this

FIGURE 5. ARRHENIUS PLOT of the hop rate of a silicon dimer along a Si substrate row versus $1/kT$, adapted from ref. 14. From the slope of the line, one deduces an activation barrier for row hopping of 0.94 ± 0.09 eV. The y -intercept at $1/kT = 0$ gives an attempt frequency of $10^{12.8 \pm 1.3}$ Hz.

dimer induce stresses in the substrate that affect the atomic-scale behavior on the surface.^{15,16} The mixed dimers adsorbed onto the Si(001) surface are only observed in the B configuration and are highly buckled, that is, one atom of the dimer is much further off the surface than the other. STM images appear to show these mixed dimers rocking just as the homogeneous Si–Si and Ge–Ge dimers do, but this is an illusion; the buckled orientation with the Ge far out of the substrate plane has a significantly lower energy than the orientation with the Ge nearer the plane and is the only orientation imaged in STM. The apparent rocking is actually a 180° rotation.¹⁷ Moreover, the rotation proceeds in stages: one atom first rotates by 90°, then the second atom rotates by 90°. The two-step process then repeats.

At temperatures for which Si–Ge dimers diffuse over a Si substrate, the Ge atom in a diffusing dimer can exchange with a substrate atom. A so-called return exchange can occur when the resulting Si–Si dimer revisits the original exchange site. Measurements of the statistical mechanical properties of such processes in heterogeneous systems, in combination with *ab initio* theoretical calculations, enable us to better understand the fundamental physics involved in surface alloy formation and growth.

The growth of semiconductor devices in common use—even simple ones—is much more complex than that of the systems we have considered in this article. In a computer chip, for example, millions of atoms are simultaneously involved in a host of competing kinetic processes. Nonetheless, much of a computer chip's surface physics can be realistically analyzed in terms of simple statistical mechanics. The results of such analyses put constraints on models that try to deduce surface behaviors from first principles and allow us to develop an intuition for the constituents of those wondrous microelectronic ensembles that enable us to process information at an ever increasing rate.

References

1. J. Dabrowski, H.-J. Müssig, *Silicon Surfaces and Formation of Interfaces*, World Scientific, River Edge, N.J. (2000).
2. H. J. W. Zandvliet, *Rev. Mod. Phys.* **72**, 593 (2000).
3. G. Brocks, P. J. Kelly, *Phys. Rev. Lett.* **76**, 2362 (1996).
4. T. Yamasaki, T. Uda, K. Terakura, *Phys. Rev. Lett.* **76**, 2949 (1996).
5. A. P. Smith, H. Jónsson, *Phys. Rev. Lett.* **77**, 1326 (1996).
6. Z. Zhang, et al., *Phys. Rev. Lett.* **74**, 3644 (1995).
7. B. S. Swartzentruber, A. P. Smith, H. Jónsson, *Phys. Rev. Lett.* **77**, 2518 (1996).
8. B. Borovsky, M. Krueger, E. Ganz, *Phys. Rev. Lett.* **78**, 4229 (1997).
9. D. W. Bassett, P. R. Webber, *Surf. Sci.* **70**, 520 (1978).
10. G. L. Kellogg, P. J. Feibelman, *Phys. Rev. Lett.* **64**, 3143 (1990).
11. C. L. Chen, T. T. Tsong, *Phys. Rev. Lett.* **64**, 3147 (1990).
12. B. Borovsky, M. Krueger, E. Ganz, *Phys. Rev. B* **59**, 1598 (1999).
13. H. J. W. Zandvliet, et al., *Phys. Rev. Lett.* **84**, 1523 (2000).
14. B. S. Swartzentruber, *Phys. Rev. Lett.* **76**, 459 (1996).
15. X. R. Qin, B. S. Swartzentruber, M. G. Lagally, *Phys. Rev. Lett.* **84**, 4645 (2000).
16. X. R. Qin, B. S. Swartzentruber, M. G. Lagally, *Phys. Rev. Lett.* **85**, 3660 (2000).
17. Z.-Y. Lu, et al., *Phys. Rev. Lett.* **85**, 5603 (2000).
18. J. M. Carpinelli, B. S. Swartzentruber, *Phys. Rev. B* **58**, R13423 (1998). ■